Development of a Continuum-Mechanics-Based Tool for 3D Finite Element Analysis of Reinforced Concrete Structures

Helmut Hartl
Institute for Structural Concrete, Graz University of Technology, Austria

ABSTRACT: A 3D (three-dimensional) finite element program has been developed for reinforced and prestressed concrete structures in order to make advanced numerical methods available to engineers. All parameters needed can be taken from the literature (codes, fib-bulletins). Concrete is modeled in terms of plasticity, employing the Ottosen failure criterion. As flow rule serves the Drucker-Prager surface. A robust return is guaranteed by the elasto-visco-plastic approach. A rotating crack model based on the cohesive crack concept is presented for tensile failure. Creep is accounted for by integrating the entire stress history. The program has the capability to account for every single rebar at its exact spatial position. The rebars are automatically discretized to the element mesh. A case study presents the interface stresses between two concrete layers due to shrinkage and creep.

1 SIGNIFICANCE OF FEM IN REINFORCED CONCRETE ENGINEERING

If the performance of a reinforced or prestressed concrete structure needs to be simulated numerically many nonlinear phenomenon will be encountered over the time and load history, even at low service load levels: shrinkage & creep, cracking and crushing at the concrete end. The reinforcement which is embedded into the concrete behaves nonlinear due to bond slip and may start to yield at high load levels.

Some tools are able to account for such nonlinear effects within a sectional analysis. Though, discontinuous regions cannot be analyzed with such tools and strut and tie models are employed in many situations of practical design. Such models show a possible flux of forces but cannot provide firm information about the serviceability. This is often an issue when an existing structure should be adapted and subjected to higher loads.

A tool for a 3D-analysis of reinforced concrete was developed (Hartl 2002a). It allows studying the interaction of several nonlinear effects of reinforced and prestressed concrete structures from the engineering point of view. No solid knowledge of the theoretical framework behind is necessary.

A successful introduction of nonlinear methods into practice can be achieved only, if these methods do require only reasonable time in order to prepare the input data. This requires that only easily accessible material parameters, which can be understood by an engineer, need to be provided on the one hand. And on the other hand the laborious work of providing the geometric input should be minimized as much as possible.

The advantage of a continuum-mechanics based approach is that nearly no simplification and idealization of the domain is necessary. Such a computer program can account by default for every single rebar at its exact spatial position. Hence, the load-bearing mechanism is computed by the program once the geometry of the domain is provided. The computing expenses are high but acceptable for today's standard computers. Considering the fast development in computer hardware, it is acceptable to increase the computing demand, if the time for preparing the input data can be decreased.

It was a major goal to develop a tool, which gains the capability to investigate soil structure interaction problems as well. In order to be able to combine some of these ideas, it appeared to be necessary that full access to the program code is available and the program should have implemented some features toward these goals. (BEFE 2001) served as a development platform. The geotechnical part is already covered by the program.

2 MATERIAL MODEL FOR CONCRETE

Concrete behavior is complex and shows a significant scatter. Several models are available for describing the constitutive behavior of concrete but none of them can be regarded as the well accepted

concrete model. Sophisticated models may be excellent for special purposes but no better results may be expected in general cases where only limited information about the concrete and the loading history is available.

The employed model is simple in concept. All parameters have a physical meaning and are familiar to an engineer.

2.1 *Concrete Crushing*

For the sake of simplicity the compressive behavior is assumed linear elastic up to the failure surface (Ottosen 1977) and perfectly plastic thereafter. This simple approach is able to describe well many engineering situations because the load deformation behavior is indeed nearly linear up to approximately 40% of f_{cm} and even more at high strength concrete. Stresses at service load level will exceed such stress levels rarely. Beyond such stress levels micro-cracks in the concrete matrix induce an anisotropic behavior and the constitutive behavior becomes rather complex. However, the ultimate stress can be described well by a failure surface.

The (Ottosen 1977) surface is described by four parameters. (Dahl 1992) proposed for the four parameters an approximation based on experimental data knowing only the compressive strength f_{cm}. The parameters computed according to Dahl can be employed for normal strength concrete and for high strength concrete. The parameters are

$$x = \frac{f_{cm}}{100[\mathrm{MN/m^2}]} \tag{1}$$

$$A = -1.66 \cdot x^2 + 3.49 \cdot x + 0.73 \tag{2}$$

$$B = -0.19 \cdot x^2 + 0.41 \cdot x + 3.13 \tag{3}$$

$$K_1 = 0.46 \cdot x^2 - 0.97 \cdot x + 11.89 \tag{4}$$

$$K_2 = -0.02 \cdot x^2 + 0.04 \cdot x + 0.974 \tag{5}$$

(ModelCode90 1993) gives recommendations for the Ottosen parameters based on the uniaxial compressive and tensile strength of normal strength concrete ($f_{ck} < 80$MPa).

If this advice is neglected, contradictory results will be obtained as shown in Figure 1. Although the uniaxial compressive strength (f_{cm} = 98MPa) is an input parameter for the failure envelope, it represents a stress state outside the failure envelope (dotted line in Figure 1). This is a clear contradiction. Therefore, the (ModelCode90 1993) recommendations should not be extrapolated for high-strength concrete. But f_{cm} is on the failure envelope if the parameters are computed according to Dahl as shown by the solid line in Figure 1.

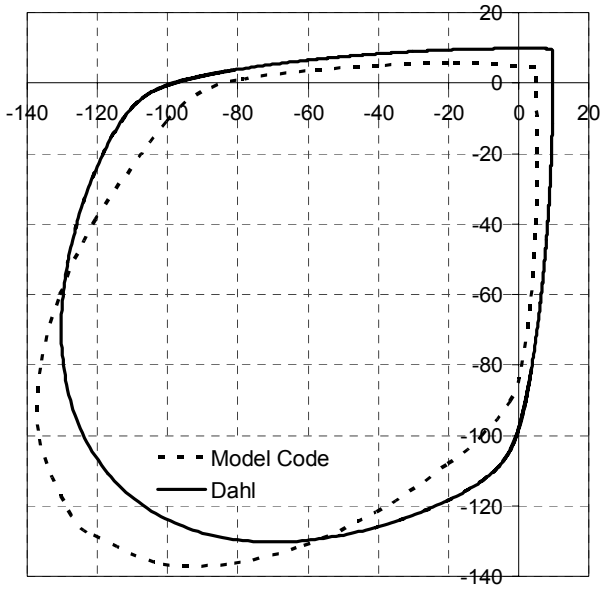

Figure 1 Ottosen envelope for C90/105 (f_{cm} = 98Mpa) with parameters according to Dahl vs. Model Code 90

A stress state outside the failure surface is not admissible. Plastic strains will develop instead and the stress state will remain on the failure surface. Therefore the computed strain increment must be split into an elastic part which may yield to another stress state on the failure surface and a plastic part which does not produce stresses. Based on experimental observations at ductile materials, it is assumed that the direction of the plastic strain increment is independent on the loading path leading to the failure envelope and on the current loading direction. Thus, a potential function may be employed as flow rule for determination of the plastic strain increment (Melan 1938). Although real concrete behavior is much more complex, the Drucker-Prager surface is employed as plastic potential function.

2.1.1 *Return algorithm*

The elasto-visco-plastic approach is employed as return method (Perzyna 1963, 1966) for its robustness. A stress state outside the yield surface is allowed for $t \neq \infty$ in this method. The stress at time $t + \Delta t$ is

$$\boldsymbol{\sigma}_{t+\Delta t} = \boldsymbol{\sigma}_t - \mathbf{D} \cdot \frac{\Delta t}{\eta} \langle F \rangle \frac{\partial Q}{\partial \boldsymbol{\sigma}} \tag{6}$$

where $\boldsymbol{\sigma}_{t+\Delta t}$ is the stress at time $t+\Delta t$. $\mathbf{D}$ is the elasticity matrix. Q is the plastic potential function, which is in this case the Drucker-Prager cone and F is the Ottosen failure criterion. $\langle F \rangle$ indicates a step function where

$$\langle F \rangle = 0 \qquad \text{if} \quad F \leq 0 \tag{7}$$

$$\langle F \rangle = f_{(F)} \qquad \text{if} \quad F > 0 \tag{8}$$

No material rheology is considered here. Thus, the viscosity parameter η is set to unity and time has no physical meaning. The time reduces to a mere convergence parameter. The plastic strain rate $\partial Q/\partial \boldsymbol{\sigma}$ is

multiplied by **D** in order to obtain the stress rate. $\Delta t \cdot \langle F \rangle$ can be interpreted as a rate multiplier $\Delta\lambda$ in order to obtain a stress state on the failure surface. This multiplier $\Delta\lambda$, which results in a limiting stress state on the yield surface, is of interest for a fast computation.

$$F_{\left(\boldsymbol{\sigma}-\mathbf{D}\cdot\Delta\lambda\frac{\partial Q}{\partial\boldsymbol{\sigma}}\right)}=0 \tag{9}$$

An analytical approach towards this issue is shown in (Mang & Hofstetter 2000). A numerical approach is shown here. The condition given (Equation 9) can be fulfilled numerically by employing an iterative scheme employing the Newton method. The derivative of F_n is approximated by means of the secant connection of two trial points as shown in Figure 2.

$$\boldsymbol{\sigma}_{n+1}=\boldsymbol{\sigma}_n-\mathbf{D}\cdot\frac{F_n}{\dfrac{F_{n-1}-F_n}{\left\|\boldsymbol{\sigma}_{n-1}-\boldsymbol{\sigma}_n\right\|}}\cdot\frac{\partial Q}{\partial\boldsymbol{\sigma}_0} \tag{10}$$

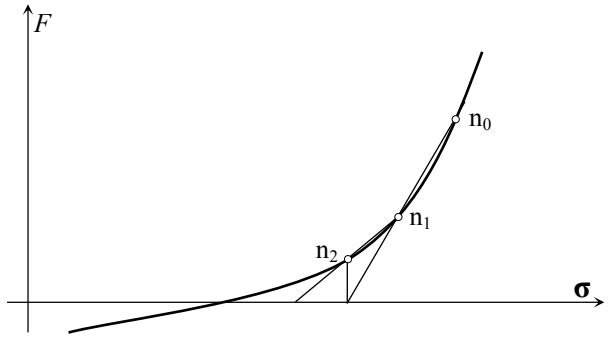

Figure 2 Iterative scheme for obtaining a stress state on the yield surface

The initial trial stress is $\boldsymbol{\sigma}_0 = \boldsymbol{\sigma}_{el}$. Then, a small value is assigned to $\Delta\lambda$ ($= \Delta t \cdot \langle F \rangle$) and $\boldsymbol{\sigma}_1$ is computed by evaluation of Equation 6. For all subsequent steps, Equation 10 applies and a fast convergence is obtained. The final stress is always on the yield surface.

A merit of this elasto-visco-plastic approach is that the derivative of the yield function F is not needed in order to compute $\boldsymbol{\sigma}$. This procedure is appealing when the derivative of the yield function is very involved and costly to compute. Only a smooth plastic potential function is required in order to ensure a robust return.

2.2 *Concrete Cracking*

Tensile cracking is a dominant source for nonlinear material behavior in reinforced concrete structures. A review of available crack models can be found in (Hofstetter & Mang 1995).

Cracking is a discrete phenomenon at discrete planes. The first crack plane is initiated perpendicular to the principal axis of any tensile stress higher than f_{ct}. Tensile stresses can be transferred still at any plane perpendicular to the crack plane. Upon subsequent rotation of the principal stress axis, the load transfer mechanism becomes complex: A certain shear stresses can be transferred still over cracks and additional crack planes may develop as well.

At reinforced concrete structures the load transfer mechanism will be controlled dominantly by the reinforcement after cracks have initiated. Hence, a sophisticated model for the shear stress transfer over open cracks seems not to be a primary issue. It is more important that the crack model accounts well for the softening behavior of cracking concrete.

The implemented crack model is formulated within plasticity theory and is based on the smeared crack concept. A crack is assumed to be smeared over the volume represented by the regarding integration point. The model accounts for the introduced anisotropy, unless the user enforces the program to assume an isotropic strength reduction.

In order to account for the anisotropy the plastic strain components (illustrated by the solid Mohr circle in Figure 3) are computed along the principal stress axis and the admissible stress for each principal axis is computed from the regarding plastic strain component. Then, an iterative procedure takes place for the stress update and additional plastic strains may arise along the principal axis. After constitutive relations are satisfied the updated plastic strain components are rotated back to the global coordinate system and stored as shown by the dashed Mohr circle in Figure 3 (Welscher 1993, Hartl 2002a).

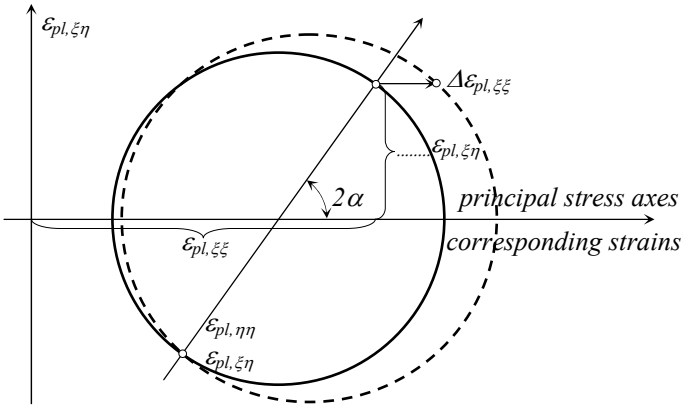

Figure 3 Update of plastic strain

Figure 4 illustrates the behavior at tensile loading. Concrete is assumed to behave linearly elastic up to the tensile limit. The user can provide a tension cut-off factor ($1.0 \geq \text{TCO} > 0.0$) in order to scale the maximum allowable tensile stress. After a certain amount of tensile flow ε_{yt} has occurred, strain-softening is accounted for in a bilinear fashion in the context of the cohesive crack concept (Hillerborg et al. 1976). There the developing crack plane is treated as discrete phenomenon. It is assumed that a certain amount of fracture energy G_F is absorbed by the formation of a unit area of crack surface. The tension softening behavior is now described by a

stress elongation diagram, which is controlled by the specific crack energy. This ensures results which are independent of the element size. The parameters for the employed model are given in Model Code 90. In the implementation the stress obtained from the model is limited such that TCO·$f_{ctm} \geq f_{ct} \geq$ rTCO·f_{ctm}.

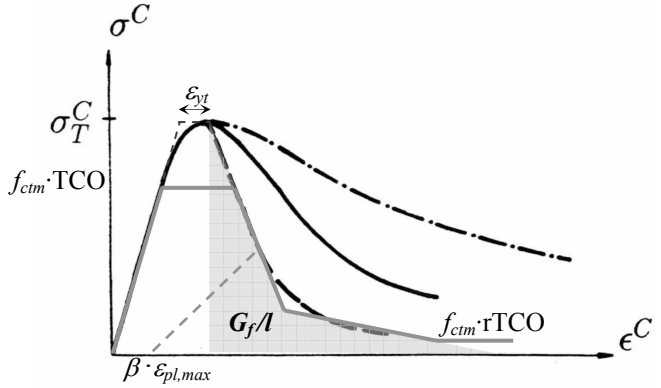

Figure 4 Constitutive behavior of a crack plane at loading and at unloading

At unloading, crack closing is taken into account by reducing the plastic strain increment and a path as illustrated by the dashed line in Figure 4 is followed. The amount of crack closing is controlled by β. An irreversible crack corresponds to $\beta = 1.0$ and a completely recoverable crack corresponds to $\beta = 0.0$. According to (Dahlblom & Ottosen 1990) $\beta = 0.20$ may give realistic results.

2.3 *Shrinkage & Creep of Concrete*

The model implemented into this work is that one of (fib bulletin No 1, 1999). This model is able to account for normal strength and for high-performance concrete. Although a model which is based on diffusion theory would be doubtless more appropriate for such a continuum based approach from the physical point of view, the model of (fib bulletin No 1) is accepted well in the engineering society and the employed parameters are simple to obtain. On the programming end, the differential equation for diffusion theory need not to be implemented. Since shrinkage is a volumetric process, the 3D shrinkage strain is

$$\boldsymbol{\varepsilon}_{sh}^T = \begin{bmatrix} \varepsilon_{sh} & \varepsilon_{sh} & \varepsilon_{sh} & 0 & 0 & 0 \end{bmatrix} \qquad (11)$$

The uniaxial shrinkage strain ε_{sh} is dependent on the cement mixture and on the environmental conditions like moisture content of the air and temperature. Creep is additionally dependent on the stress history of the concrete. Procedures which do not require storage of the entire stress history are discussed in (Hofstetter & Mang 1995). However, the respective algorithms are not able to account for the general case and are therefore disregarded. The additional computing expenses (especially storage and CPU) for accounting for the entire stress history are no longer genuine computational challenges.

The stress history is approximated on the basis of an implicit midpoint rule as shown in Figure 5 and in Equation 12, (Walter 1988, Hofstetter&Mang 1995).

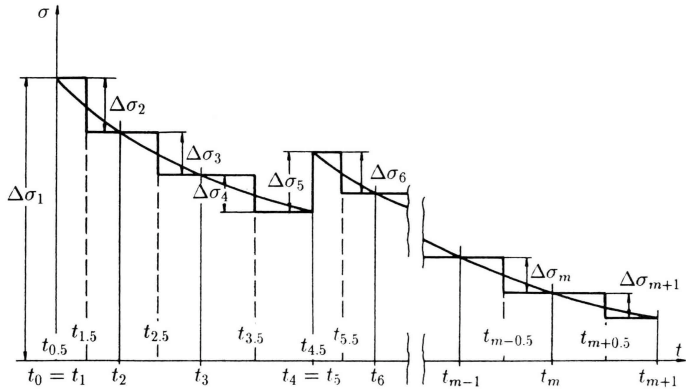

Figure 5 Approximation of the stress history by an implicit integration.

$$\boldsymbol{\varepsilon}_{cc}\left(t_m\right) = \mathbf{A} \cdot \sum_{i=1}^{m} \frac{\varphi\left(t_m, t_{i-1/2}\right)}{E_{ci}} \Delta\boldsymbol{\sigma}\left(t_i, t_{i-1}\right), \quad m \geq 2 \qquad (12)$$

No recommendation could be found in literature for the Poisson's ratio of the creep compliance matrix. According to (Bažant/Wittmann 1982), ν_{cr} may drop almost to zero. If no better value for ν_{cr} is available, $\nu_{cr} = 0.20$ might serve as an acceptable but crude first approximation.

Figure 6 shows the development of creep coefficients for one concrete loaded at different ages.

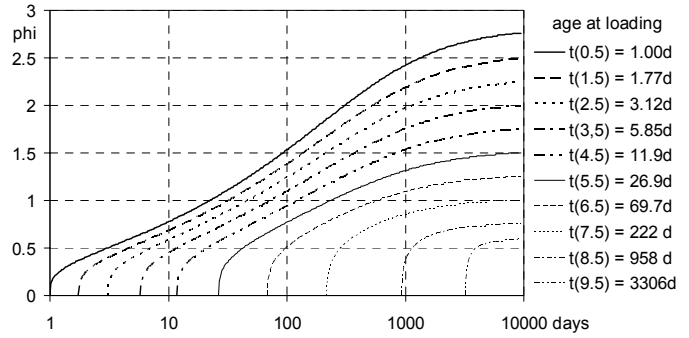

Figure 6 Development of creep coefficients for a generic concrete

At stress levels above a certain limit the relation between stresses and creep strains is no longer linear. For stresses between 0.40·f_{cm} and 0.60·f_{cm}, the regarding creep coefficients are modified depending on the current stress level according to Model Code 90.

3 MODELLING THE REINFORCEMENT

The reinforcement represents a discontinuity of the stiffness distribution within a reinforced concrete member. Only in very few cases the domain is subdivided into plain concrete elements and steel elements. This will be done only, if details are investigated.

In general, a formulation needs to be employed which is able to account for both, the concrete and the reinforcement in an implicit manner.

The embedded formulation of the reinforcement accounts for the exact geometric position of the reinforcement without giving any restriction to the element mesh of the concrete as shown in Figure 7.

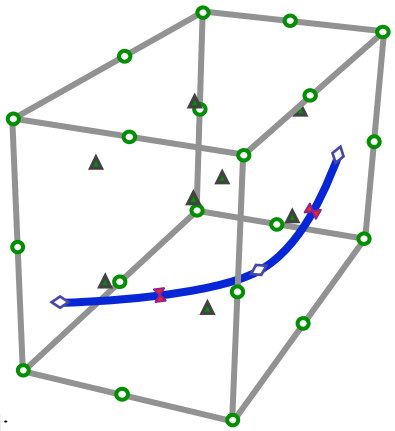

Legend:

- Node of parent element; (DOF, appears in the vector of nodal element displacements)
- Rebar point; (does not appear in the vector of nodal element displacements)
- Integration point for the parent element; (local coordinates of the Gauss points are known)
- Integration point for the rebar; (local coordinates and rebar orientation have to be determined)

Figure 7 Embedded reinforcement bar

The mesh of the parent domain can be prepared independently of the reinforcement layout. The reinforcement needs to be provided in global coordinates only. A preprocessing routine detects automatically the intersection of the rebars with the parent element faces, (Hartl 2002a). And the rebar stiffness is added to the concrete stiffness in the element stiffness matrix.

$$\mathbf{K}^e = \int_{parent} \mathbf{B}^{eT} \mathbf{D}_c \mathbf{B}^e \cdot dV + \int_{rebar} \mathbf{B}^{eT} \mathbf{T}^T_{\varepsilon,gl} \mathbf{D}_r \mathbf{T}_{\varepsilon,gl} \mathbf{B}^e \cdot dV \quad (18)$$

The crux in this method is that the integration points of the reinforcement need to be found in local coordinates of the parent elements. This inverse mapping is not straightforward, a Newton root finding algorithm in three dimensions needs to be applied in order to find these integration points for the rebar within the parent element.

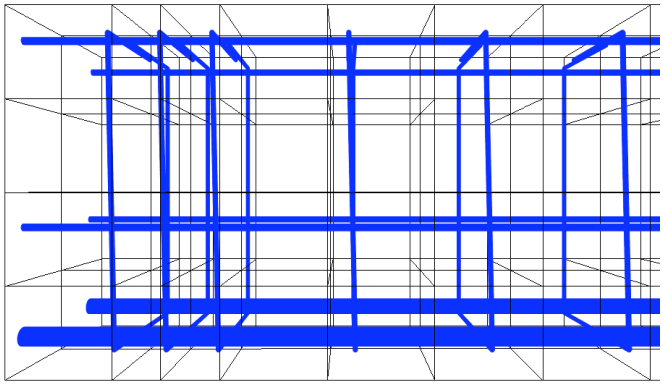

Figure 8 Concrete mesh and embedded reinforcement

Figure 8 shows a concrete mesh with embedded rebars. The effort for preparing the input in this way is small. Modifications can be made in a simple way.

4 CASE STUDY, STRESS AT THE INTERFACE OF TWO CONCRETES

Bridge decks are exposed to traffic and environmental aggression. The concrete cover is removed often during general repair work by high pressure water jetting. In order to enhance the deck for increased traffic loads a new concrete layer with a certain thickness is often cast on top of the existing deck. The load transfer mechanism and the bearing behavior was investigated experimentally by (Kernbichler 2002a, b) and numerically by (Hartl 2002b).

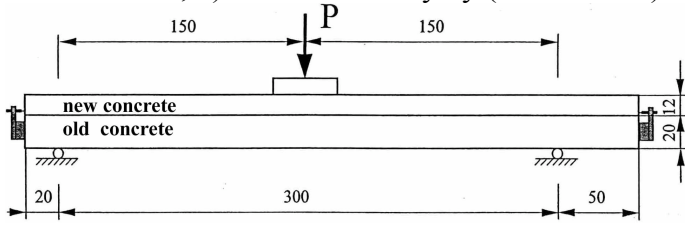

Figure 9 Setup of the experiment, depth of plate 2.50m

The setup of the test is shown in Figure 9. Let us concentrate here on the development of stresses due to shrinkage and creep of these two concretes with different ages. A considerably tensile stress exists at the bottom after the old concrete has experienced creep and shrinkage over 25 years since the reinforcement obstructs the shorting caused by shrinkage as shown in Figure 10a for the right end of the plate. The normal stresses are almost zero at the top of the old concrete since the reinforcement ratio is much lower at the top. The normal stresses in the newly installed concrete are obviously zero at 25 years.

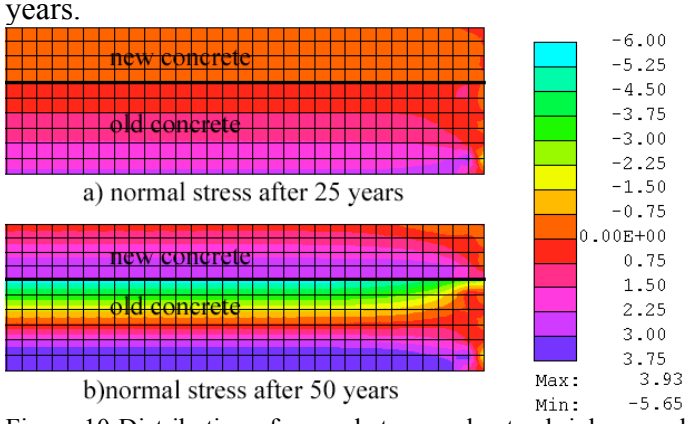

Figure 10 Distribution of normal stresses due to shrinkage and creep.

Figure 10b shows the stress distribution when the new concrete is 25 years old (then the old concrete is 50 years old). The new concrete has high tensile stresses and the old concrete has compressive stresses close to the interface.

Shear stresses up to 2MN/m² arise after 50years in the interface between these two concretes without

any external load acting as shown in Figure 11 for the right end of the plate. Considering this situation on a Mohr circle, the according principal stress has the same magnitude and is obtained by rotating the axis by 45° since the stress perpendicular to the interface is zero. (Daschner 1976) observed that concrete develops at a well prepared interface almost the same strength as monolithic concrete. Assuming $f_{ctm} \approx 3MN/m^2$ for the given situation, the shear stress in the interface is utilized at about 2/3 of its ultimate capacity close to the outer end of the plate. And upon loading, the shear stress does not increase in this region as shown in Figure 11b for P = 1000kN.

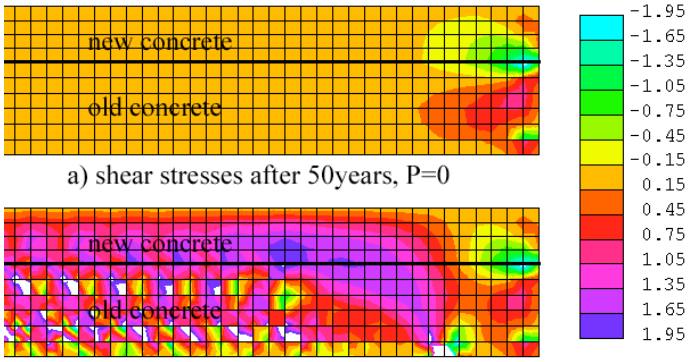

a) shear stresses after 50years, P=0

b) shear stresses after 50years, P=1000kN

Figure 11 Shear stress after 50 years due to shrinkage and creep

5 CONCLUSION & OUTLOOK

The developed program is applied with success in several areas.

- Laboratory tests are reanalyzed with the program for two purposes. On the one hand to get more insight into the structural behavior especially at parameter variations. And, on the other hand to validate the computer program itself.
- It is in use as well in teaching for graduate students. The students get fast familiar with the program and they are able to study the load bearing behavior of a detail as part of their advanced concrete class.
- For consulting in special cases.

Additional non nonlinear phenomena of reinforced concrete are implemented into the code as these phenomena appear to be an issue in a case study. However, an additional plan is to make many of the described and well tested features available to standard FE-codes, like Abaqus or similar ones by means of user routines.

REFERENCES

Bažant Z.P., Wittmann F.H., (eds.) 1982, *"Creep and shrinkage in concrete structures"*, John Wiley & Sons, New York

BEFE 2001: Beer G., *"BEFE user's reference and verification manual"*, CSS, Graz

Dahl K.K.B., 1992, *"A failure criterion for normal and high strength concrete"*, Technical University of Denmark, Lyngby

Dahlblom O., Ottosen N.S., 1990, *"Smeared crack analysis using generalized fictitious crack model"*, Journal of Engineering Mechanics, 116, pp. 55-76

Daschner F., 1986, *"Versuche zur notwendigen Schubbewehrung zwischen Betonfertigteilen und Ortbeton"*, Deutscher Ausschuß für Stahlbeton, Heft 372, Ernst&Sohn, Berlin

Elwi A.E., Hrudey T.M., 1989, *"Finite element model for curved embedded reinforcement"*, Journal of Engineering Mechanics, 115, pp. 740-754

fib bulletin No 1, 1999, *"Structural concrete"*, vol. 1, International Federation for Structural Concrete (fib), Lausanne

Hartl H., 2002a, *"Development of a Continuum-Mechanics-Based Tool for 3D Finite Element Analysis of Reinforced Concrete Structures and Application to Problems of Soil-Structure Interaction"*, Doctoral Thesis, Graz University of Technology, Austria

Hartl H., Sparowitz L., 2002b, *"A 10 Tauernautobahn, Brückenverstärkung F8/F8a und F9, Numerische Untersuchung des Tragverhaltens nachträglich ergänzter Stahlbetonplatten"*, Institute for Structural Concrete, TU-Graz, Graz

Hillerborg A., Modeer M., Peterson P.E., 1976, *"Analysis of crack formation and crack growth in concrete by means of fracture mechanics and finite elements"*, Cement and Concrete Research, 6, pp. 773-782

Hofstetter G., Mang H.A., 1995, *"Computational mechanics of reinforced concrete structures"*, Vieweg, Braunschweig

Kernbichler K., 2002a, *"A10 Tauernautobahn / Brückenverstärkung F8 / F8A und F9: Bericht über experimentelle Untersuchung des Tragverhaltens nachträglich ergänzter Stahlbetonplatten"*, Konstruktive Versuchsanstalt, Graz University of Technology, Graz

Kernbichler K., 2002b, *"A10 Tauernautobahn / Brückenverstärkung F8 / F8A und F9: Bericht über ergänzende experimentelle Untersuchung des Tragverhaltens nachträglich ergänzter Stahlbetonplatten"*, Konstruktive Versuchsanstalt, Graz University of Technology, Graz

Mang H., Hofstetter G., 2000, *"Festigkeitslehre"*, Springer, Wien

Melan E., 1938, *"Zur Plastizität des räumlichen Kontinuums"*, Ingenieur-Archiv, **9**, pp. 116-126

Model Code 90, 1993, *"CEB-FIP model code 1990"*, CEB-FIP Comitè Euro-International du Bèton, Thomas Telford, London

Ottosen N.S., 1977, *"A failure criterion for concrete"*, Journal of the Engineering Mechanics Division, 103, pp. 527-535

Perzyna P. 1963, *"The constitutive equations for rate sensitive plastic materials"*, Quarterly of Applied Mathematics, **20**, pp. 321-332

Perzyna P., 1966, *"Fundamental problems in viscoplasticity"*, Advances in Applied Mechanics, **9**, pp. 243-377

Walter H., 1988, *"Finite Elemente Berechnungen von Flächentragwerken aus Stahl- und Spannbeton unter Berücksichtigung von Langzeitverformungen und Zustand II"*, Doctoral Thesis, TU-Vienna, Vienna

Welscher S., 1993, *"Implementierung und Anwendung eines elasto-plastischen Werkstoffmodells für Beton"*, Master Thesis, Institute for Strength of Materials, TU-Vienna, Vienna,